PHYSICAL REVIEW A VOLUME 20, NUMBER 6 DECEMBER 1979

Electric field dependence of the photoionization cross section of Rb

Richard R. Freeman and Nicholas P. Economou
Bell Laboratories, Holmdel, New Jersey 07733
(Received 27 April 1979)

The relative photoionization cross section of ground-state Rb is measured near threshold as a function of applied electric field strength. The cross section is found to have a wavelength-dependent resonance structure that changes with the strength of the electric field. This resonance structure is observed not only for energies above the classical field ionization limit, but for the case of π excitation, beyond the zero-field ionization limit as well. An analysis of the data is presented that connects the concepts of "strong-field mixing" and the perturbation calculations of the energies of hydrogenic Stark components.

I. INTRODUCTION

There has recently been a great deal of interest in the spectroscopy of atomic systems in extreme values of external fields for which the motion of the optically active electrons is determined equally by the Coulomb field and the applied external fields. This general problem has been termed "strong-field mixing,"[1] and several authors have treated the cases of Coulomb plus magnetic fields[2] and Coulomb plus electric fields.[3] Interest in these phenomena received its impetus from the observations by Garton and Tomkins of quasi-Landau resonances in the absorption spectrum of Ba in high magnetic fields,[4] and several groups have studied the Coulomb plus magnetic field case experimentally in several atoms using a variety of techniques.[5] More recently, the problem of atomic systems in intense electric fields has been investigated,[6] and Freeman *et al.*[7] have experimentally observed the positive energy resonances in the Coulomb plus electric field case that are analogous to the quasi-Landau resonances in the Coulomb plus magnetic field case.

In the case of the Coulomb plus electric field, the phenomenon of field ionization plays an important role, and near the field-ionization threshold, the Coulomb plus electric field problem has received considerable attention, both experimentally[8] and theoretically.[9] Littman *et al.*[10] and Feneuille and Jacquinot[11] have discussed the role of ionization in the spectroscopy of Stark states near the classical ionization threshold. The understanding of field-ionization behavior of alkali-metal atoms *vis-a-vis* hydrogen is now a subject of current investigation.

We present here the details of the measurements of the photoionization cross section of ground-state rubidium in the presence of various strengths of applied electric field that were originally reported in Ref. 7. In Ref. 7 attention was drawn primarily to the positive energy resonances. Our purpose in this paper is to identify the majority of the structure in the observed photoionization cross section for a much wider range of energies. In the process we show how the semiclassical strong-field mixing analysis merges with calculations of energy levels of hydrogenic Stark components using standard perturbation techniques.

II. EXPERIMENTAL

In the presentation of the results, and in the subsequent discussion, we refer to "photoionization" in its generic form: the neutral ground-state atom absorbs a photon of energy hc/λ and emits an electron *within the observation time*. This definition includes the conventional, field-free photoionization that is energetically possible only above the zero-field ionization limit. In addition, it includes the excitation and subsequent field ionization of any Stark component in the electric field whose lifetime against ionization is less than or equal to the observation time. Unlike experimental techniques in which the observation interval timing is adjusted to isolate specifically different field ionization rates,[10] we have a constant timing window that records all levels whose ionization rate exceeds approximately 5×10^4 sec^{-1}.

The single-photon photoionization yield of Rb in the presence of various values of a constant, uniform electric field was obtained between approximately 3005 and 2960 Å using a doubled pulsed-dye laser of bandwidth 0.5 cm^{-1}, a collision-free atomic beam, and appropriate electronic laser-intensity normalization procedures. The relevant experimental details have been given previously.[7] Considerable effort was expended to insure that the recorded wavelength dependence of the photoionization yield was independent of laser intensity, atomic beam density, electronic gain or position of excitation of the atomic beam within the apparatus. We esti-

mate the electric field to have been uniform over the excitation volume to better than 1 part in 10^3. In all cases studied, the photoionization ion current was observed to be linear in the uv laser intensity.

The relative photoionization yield for π polarization (laser E field parallel to applied field) as a function of wavelength is shown in low resolution for four values of the electric field in Fig. 1. At the positions marked, the gain has been changed and the zero signal level offset by the indicated amount. For each field value, the relative photoionization yield indicated on the figure is accurate, while the scale for different field values is arbitrary. At zero field (not shown in Fig. 1) a Rydberg series of $5s \rightarrow np$ resonances terminating on the zero-field ionization limit was observed. For all values of the field, π polarization cross sections show a regular, systematic variation in magnitude, with modulations that extend beyond the zero-field ionization limit. With increasing values of the field, the modulations above the zero-field limit become increasingly more pronounced (having a modulation depth of nearly 25% at 6416 V/cm, the largest field used in this study).

In Fig. 2 a comparison of σ (laser E field perpendicular to applied field) versus π polarization for the photoionization yield of Rb at 4335 V/cm is shown. What is evident in this figure was found to be the case for all field values studied: for σ polarization the photoionization cross section loses the resonance-like structure at energies well below the zero-field ionization limit. For energies near and above the zero-field limit the σ excitation cross section appears to be smooth and structureless, even at enhanced gain settings.

III. DISCUSSION

A. Resonances above the zero-field limit

In Ref. 7, attention was drawn to the fact that, from a classical standpoint, resonance structure for positive energies in the case of Coulomb plus electric field potential can result from quasi-periodic electron orbits which are tightly constrained along the z axis on the "cathode" side of the nucleus. In these orbits the electron simply misses the escape route over the reduced potential hill on the "anode" side of the nucleus and can undergo cyclical motion that is surprisingly stable.

An illustration of the classical motion of these

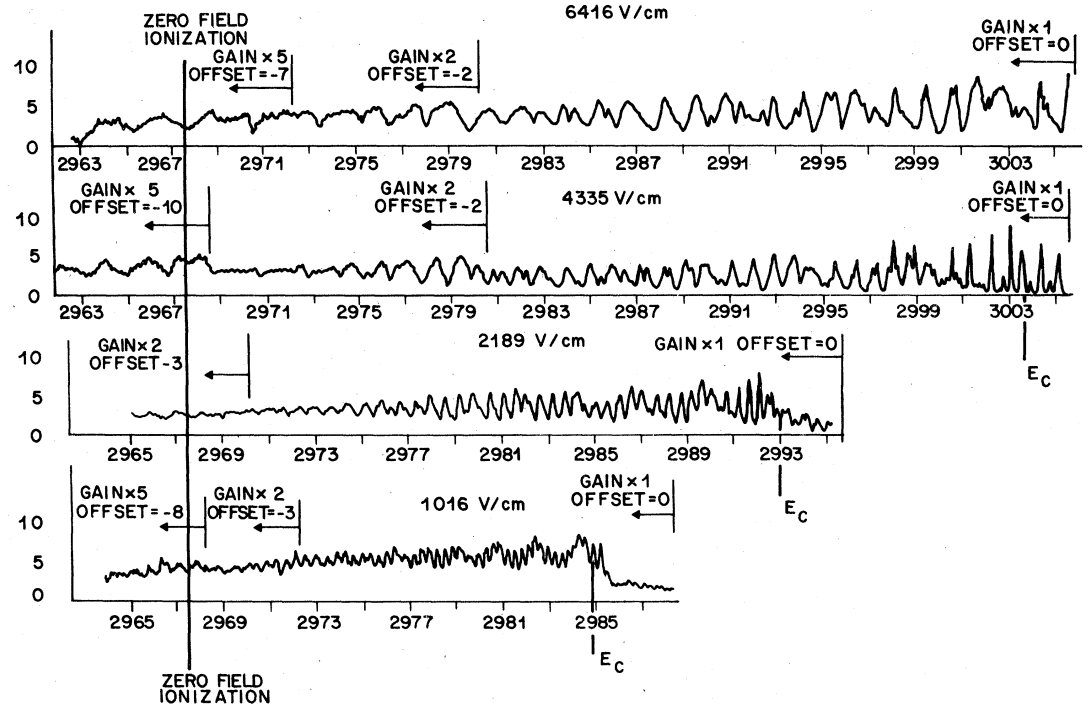

FIG. 1. Relative photoionization cross section of Rb in various strengths of electric field for light polarized parallel (π polarization) to the applied field. Note the gain and offset changes. The zero-field ionization limit, as well as the "classical field-ionization threshold" given by Eq. (1), is marked. The relative photoionization yield for a given field is accurate, while the scale for different fields is arbitrary.

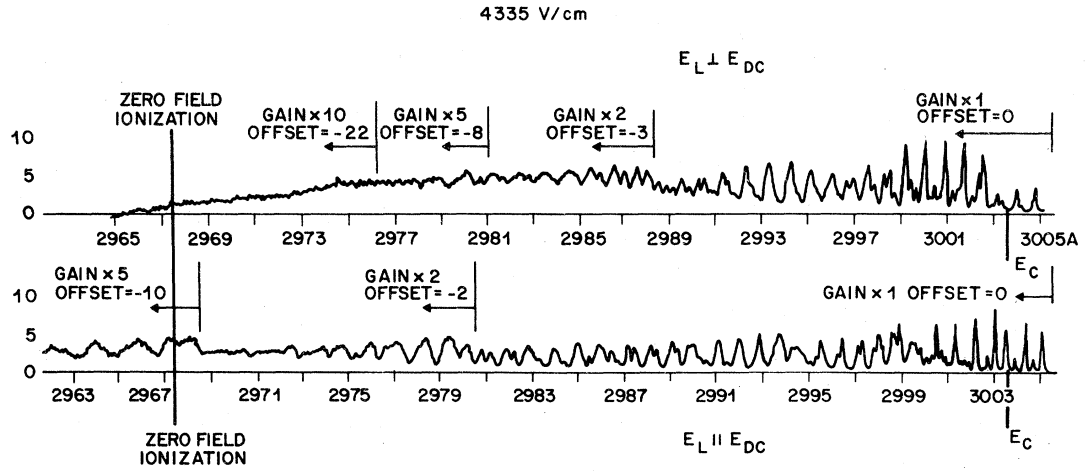

FIG. 2. Comparison of the photoionization cross section for π ($E_L \parallel E_{DC}$) and σ ($E_L \perp E_{DC}$) polarizations. What is evident in this figure was found to be the case for all field values: for energies near to and above the zero-field limit, the σ excitation cross section is smooth and structureless, even at enhanced gain settings.

orbits is given in Figs. 3(a) and 3(b). In Fig. 3(a) the result of a numerical orbit calculation is given where the electron starts at rest approximately 760 Å from the nucleus and 100 Å from the z axis in the total potential of a Coulomb field of charge +1 and an external field of 3000 V/cm. The total energy of the electron is +32.7 cm^{-1}; that is, positive energy motion corresponding to excitation above the zero-field ionization limit. In Fig. 3(b) the result of the calculation is given for the same conditions, only the initial distance of the electron from the z axis is 25 Å. These results show

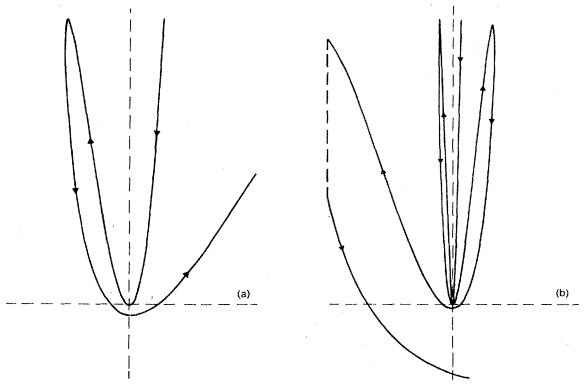

FIG. 3. (a) Results of a numerical orbit calculation of the classical trajectory of an electron moving in the total potential of a point-charge nucleus (at intersection of dotted lines) and an external field. In this figure the electron starts from rest 760 Å from the nucleus and 100 Å from the z axis, in a field of 3000 V/cm (pointing from top to bottom) with a total energy of +32.7 cm^{-1} (i.e., positive total energy). (b) Same calculation, except the starting point of the electron is moved closer to the z axis by a factor of 4.

that as the electron's initial position is placed closer to the z axis, the electron passes the nucleus a greater number of times before it escapes to the anode and "ionizes."

The calculations of Figs. 3(a) and 3(b) also point out the origin of the differences between cross sections obtained above the zero-field limit for σ and π polarizations. The stable orbits occur for motion tightly constrained along the z axis: these orbits are the classical analog of quantum states which have no angular momentum about the z axis, that is, $m_l = 0$. Since the ground state of Rb is $m_l = 0$, only π polarized light can be used to excite these classically quasiperiodic orbits.

From the results presented in Figs. 3(a) and 3(b), quasiperiodic motion of the electron results from essentially one-dimensional motion along the cathode side of the nucleus. The quantum condition for this classical motion can be constructed by imposing Bohr-Sommerfeld quantization on the one-dimensional potential $V = -e^2/|Z| - eFZ$ for $Z < 0$. This is the method used in Ref. 7. The agreement of this calculation with the experimentally observed locations of the resonances and their dependencies upon the applied field is excellent. (A fully quantum-mechanical treatment of the photoionization of hydrogen in an external electric field has been recently given by E. Luc-Koenig *et al.*[12])

Rau[13] and Lu[14] have pointed out that if one uses the parabolic coordinate system in which the Coulomb plus electric potential is separable,[15] then, for $m_l = 0$,[16] the electron experiences binding in the ξ direction and no binding in the η direction. (There is a formal analogy here to autoionization, in which a bound configuration is degen-

erate with a continuum configuration, and there exists a coupling between them. Here the "coupling" between the ξ and η coordinates arises from the restrictions on the two separation parameters, Z_1 and Z_2, namely $Z_1+Z_2=1$).[13] If the Bohr-Sommerfeld quantization condition is applied to the $m_l=0$ effective potential in ξ, $V(\xi)=-Z_1e^2/\xi+\frac{1}{8}eF\xi$, a closed expression for the spacing of the resonances at $E=0$ can be derived[17]:

$$dE/dn=(22.5\ \mathrm{cm}^{-1})(F/4335\ \mathrm{V/cm})^{3/4}.$$

This expression is in excellent agreement with the results shown in Fig. 1. This $F^{3/4}$ scaling of the resonances is characteristic of strong-field mixing and differs significantly from the F^1 scaling of the weak-field perturbation limit or the $F^{2/3}$ scaling of the triangular potential well.[18] This quasi-one-dimensional Coulomb plus electric potential in a free atom finds its analogs in other, more complicated physical systems; for example, quantum levels in a one-dimensional image Coulomb potential seen by electrons in electron layers at the surface of liquid helium.[19]

B. Resonance structure above the classical field-ionization limit

The "classical field-ionization limit" is the field value for which a state of energy E lies higher in energy than the value of the potential at the local maximum on the anode side of the nucleus. The value of the field for this condition is

$$F_{\mathrm{cl}}=\tfrac{1}{4}E^2. \tag{1}$$

Using the zero field energy of $E=-1/2(n^*)^2$ (where n^* is the effective quantum number of the state), Eq. (1) gives the familiar $F_{\mathrm{cl}}=1/(2n^*)^4$.

As discussed in more detail below, Eq. (1) has no relevance in pure Coulomb plus electric potential problems, but it does play a role when the Coulomb potential is modified at distances near the nucleus by the "core" electrons in an alkali-metal atom. In Figs. 1 and 2, the position marked E_c is calculated from Eq. (1). In Fig. 4 a simplified energy versus field diagram for the hydrogenic Stark manifolds of principle quantum number $n=22$ and 24, calculated by fourth-order perturbation theory, is shown. The results of Eq. (1) are also shown: if Eq. (1) were correct, all the states would be continuum states for energies greater than $-|E_c|=-2\sqrt{F_0}$ where F_0 is the applied field. Note that in Fig. (1) a rather well-defined increase in an underlying smooth component in the photoionization yield is observed for energies just above $|E_c|$.

For the pure Coulomb plus electric potential (i.e., the hydrogen atom in an electric field), the expression for $|m_l|=1$ (and also approximately

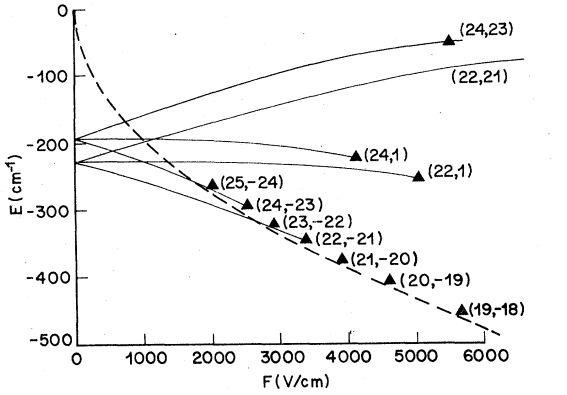

FIG. 4. Plot of energy vs field for several Stark components of various principle quantum number n. The dotted line is the "classical ionization field" according to Eq. (1); the triangular symbols are the field ionization values for the individual components according to Eq. (2). The energies of the states $(n, n_1-n_2, m_l=0)$ are calculated according to fourth-order perturbation theory.

for $m_l=0$) is given by

$$F_{\mathrm{cl}}=(E)^2/4Z_2, \tag{2}$$

where both E and Z_2 (≡ separation parameter associated with the η equation in parabolic coordinates[15]) depend upon the field. Although Eq. (2) correctly accounts for the different energies of various Stark components in the field, it does not admit tunneling and thus is properly labeled "classical."

Equation (2) predicts, in contrast to Eq. (1), that each Stark component belonging to a principle quantum number n should have a different classical limit; indeed Z_2 varies from approximately 1 (the "reddest" component, corresponding to wave functions extended out toward the anode) to approximately $1/n$ (the "bluest" component, corresponding to wave functions extended out toward the cathode). In Fig. 4, some representative Stark components are marked by their classical ionization limits according to Eq. (2). For example, at 2189 V/cm all components of $n=22$ and 24 have classical ionization fields given by Eq. (2) which are greater than predicted by Eq. (1) and, indeed, greater than 2189 V/cm. Thus, it seems natural to expect that the sharp, resonancelike structure in the photoionization yield at energies greater than E_c (in Figs. 1 and 2) are individual Stark components which are: (a) unbound continuum states according to Eq. (1); (b) perfectly stable Stark states according to Eq. (2); but, are really (c) tunneling, quasi-stable Stark components whose ionization rates are at least $5\times10^4\ \mathrm{sec}^{-1}$. (Feneuille and Jacquinot[11] have given a similar discussion in analyzing the results of Ref. 6 for sharp resonances observed just above the classical ionization limit.)

In Fig. 5 we show a scan of the π polarization cross section for 2189 V/cm between 2995 and 2978 Å using an expanded wavelength scale. On this figure the locations of the hydrogenic Stark components $(n, n_1 - n_2, m_l = 0)$ calculated from fourth-order perturbation theory[20] are shown. The agreement between the experimental results and hydrogenic Stark-effect calculations in this spectral region of the photoionization cross section is quite good.

This apparently contradictory result, that the simple picture of field ionization represented by Eq. (1) predicts the onset of a continuum background, although the resonance structure on top of this background is predicted by Eq. (2), has been discussed previously.[10] On Fig. 4 the dotted line represents Eq. (1), while the ionization limits for the reddest components of several n according to Eq. (2) are also marked. Note that these limits fall nearly along the dotted line. This is because for the reddest components, $Z_2 \simeq 1$, so Eq. (2) becomes Eq. (1) if the correct (Stark-shifted) values of E are used. Because of the core electrons in an alkali-metal atom, various Stark components belonging to different principle n manifolds do not cross. The relatively stable blue components of a lower n are coupled to the fast ionizing red components of higher n as they approach the fields represented by the dotted line on Fig. 4. Thus any Stark state will pick up a minimum ionization rate at field F when its energy satisfies $|E| = +2\sqrt{F}$. In their study of lithium, Littman *et al.*[10] showed this minimum rate to be at least 10^5 sec^{-1}. In our case, at the energies greater than E_c given by Eq. (1) (and marked in Figs. 1, 2, and 5), the ionization rate for all states is at least 5×10^4 sec^{-1}, which is the minimum rate necessary in order for us to detect the state. However, the details of the higher ionization rates depend upon the particular state.

Since the linewidth of the laser was approximately 0.5 cm^{-1} (yielding an instrument resolution given by the essentially isolated line at 2991.45 Å (19, 12, 0), and because most of the structure arises from an experimental convolution of several Stark components, no extraction of the energy widths of the individual components was attempted. Although the hydrogenic Stark-effect theory approximately locates the resonance positions in this wavelength region of the cross section, the widths and intensities of these

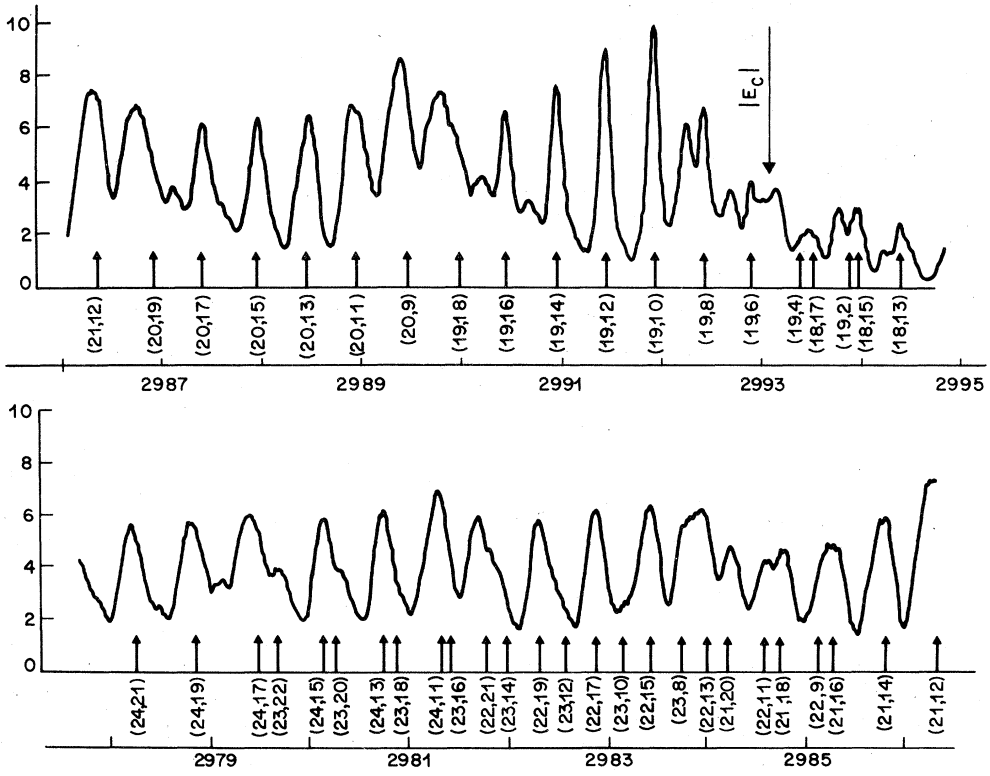

FIG. 5. Expanded wavelength-scale sweep of the photoionization cross section of Rb for an external field value of 2189 V/cm between 2995 Å and 2978 Å. Also plotted are the energies of the Stark components $(n, n_1 - n_2, m_l = 0)$ calculated by fourth-order perturbation theory for 2189 V/cm.

resonances probably depend sharply on the details of the interactions of the core electrons with the valence electron.

For wavelengths shorter than about 2978 Å, the resonance structure observed at 2189 V/cm (see Fig. 1), begins to broaden noticeably. From 2978 Å to the zero-field ionization limit at 2967.5 Å the resonance structure weakens and broadens. In addition, the fourth-order hydrogenic Stark theory becomes increasingly less accurate in predicting the location of the resonances. This is not surprising, for it is known that Stark-effect perturbation theory fails to converge at high enough order for any n and field value,[21] and will certainly diverge in fourth order for a large enough field or n. Table I shows the prediction for the bluest lines of several n values for successive orders up to fourth at $F = 2189$ V/cm.

C. Analysis of structure in the photoionization yield near the zero-field ionization limit

In this section we analyze the structure observed in the cross section for 2189 V/cm between approximately 2980 Å and a zero-field ionization limit at 2967.5 Å. In this region neither the one-dimensional analysis (used in Sec. A above for the positive energy resonances) nor the perturbation calculations of the Stark effect in hydrogen (used in Sec. B above for the resonances near the classical field ionization energy) is sufficient by itself to predict the observed structure.

The starting point of the analysis is to note that the Bohr-Sommerfeld quantization condition applied to the effective potential in ξ (or equivalently to the model potential as in Ref. 7) approximately calculates the energy of the bluest Stark component of principle quantum number n where $n = n_r + 1$ and n_r is in the equation:

$$\int_0^{\xi_0} \left(\frac{2M}{\hbar^2}(E - V(\xi))\right)^{1/2} d\xi = (n_r + \tfrac{1}{2})\pi \,. \tag{3}$$

This calculation is increasingly more accurate as n increases. This is because the neglect of the η coordinate becomes less important as the ratio of the parabolic separation parameters, Z_1/Z_2, becomes $\gg 1$. As noted above, for the bluest component, this ratio is approximately n, so that near the zero-field ionization limit, where n calculated from the one-dimensional analysis is about 30, Eq. (3) yields an excellent approximation to the Stark energy of the bluest components. In Table II we show a comparison of the one-dimensional analysis and fourth-order perturbation theory for various n with the data for 2189 V/cm. In Fig. 6 the photoionization yield from 2974 to 2966 Å is shown, with the predictions for the bluest Stark component for $n = 26$ to 32 given in row A by the one-dimensional analysis, and in row B by fourth-order perturbation theory. For $n = 26$ to 32 the one-dimensional analysis correctly labels the bluest Stark component, while the perturbation calculation becomes increasingly more inaccurate. For lower n where the perturbation expansion converges (see Table I), the perturbation calculation is in agreement with the data while the one-dimensional analysis is progressively less accurate as n decreases.

Figure 6 suggests that the substructure in the photoionization cross section near the zero-field ionization limit is due to components other than the bluest ones. For example, the substructure at 2967.5 Å (the ionization limit) is probably the Stark component (32, 29, $m_l = 0$), while the sub-

TABLE I. First through fourth-order perturbation calculation of energy of "bluest" component of principle quantum number n in a field of 2189 V/cm.

n	$(n_1 - n_2)$	$E1$	$E2$	$E3$	$E4$
18	17	−295.83	−297.05	−296.93	−296.95
19	18	−256.08	−257.76	−257.55	−257.59
20	19	−221.12	−223.40	−223.06	−223.14
21	20	−190.02	−193.07	−192.51	−192.67
22	21	−162.03	−166.06	−165.17	−165.48
23	22	−136.59	−141.84	−140.45	−141.03
24	23	−113.22	−119.99	−117.86	−118.92
25	24	−91.57	−100.21	−97.00	−98.88
26	25	−71.32	−82.25	−77.49	−80.75
27	26	−52.24	−65.93	−58.99	−64.52
28	27	−34.12	−51.14	−41.14	−50.35
29	28	−16.79	−37.79	−23.57	−38.62
30	29	−0.12	−25.83	−5.86	−30.06
31	30	+16.02	−15.27	+12.48	−25.82

TABLE II. Comparison with data of prediction of "bluest" component of principle quantum number n by fourth-order perturbation theory and one-dimensional analysis: $F = 2189$ V/cm.

n	$n_1 - n_2$	E(perturbation theory)	E(model)	Data
20	19	−223.14	−117.0	−223.0
21	20	−192.67	−189.0	−193.0
22	21	−165.48	−162.0	−165.5
23	22	−141.03	−138.0	−141.0
24	23	−118.92	−117.0	−119.0
25	24	−98.88	−96.0	−99.0
26	25	−80.75	−78.0	−79.0
27	26	−64.52	−59.0	−57.0
28	27	−50.32	−42.0	−43.0
29	28	−38.62	−25.0	−25.0
30	29	−30.06	−12.5	−12.0
31	30	−25.82	+1.2	+1.5

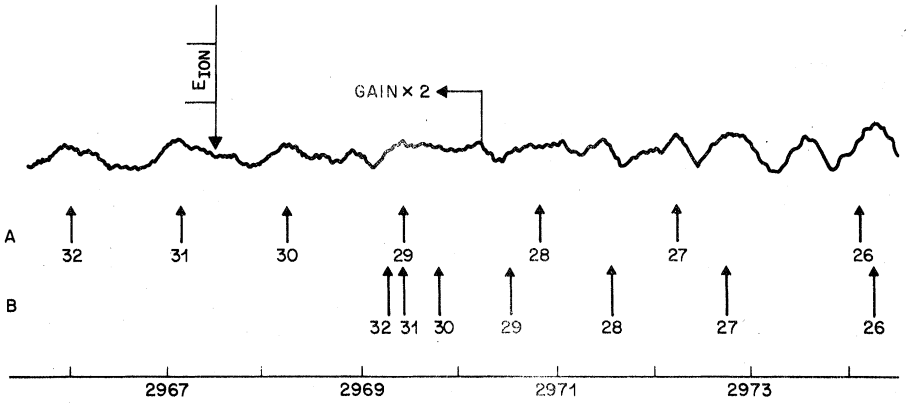

FIG. 6. Expanded scale sweep of the photoionization cross section of Rb for an external field value of 2189 V/cm between 2974 and 2966 Å. In row A, the "strong-field-mixing" calculation of the bluest component of principle quantum n is shown. In row B, the fourth-order perturbation calculation of the bluest component of the same states is shown.

structure next to (32, 31, $m_l = 0$) is probably (33, 30, $m_l = 0$).

IV. CONCLUSION

We have presented an analysis of the origins of the structure in the photoionization cross section of ground-state rubidium in the presence of an externally applied electric field. The following are major results of our analysis.

(i) The positive energy resonances observed in the cross section are shown to be reasonable from a classical point of view. Further, these resonances are shown to be quantum states which correspond to the electron's being predominantly on the cathode side of the nucleus. These states have atomic dipole moments oppositely oriented to the field and thus have large positive Stark shifts. The one-dimensional calculation presented here provides an accurate prediction of the energies of these states, even when the conventional perturbation calculation diverges.

(ii) The energies of the resonances riding on top of the continuum structure in the cross section are predicted, over a wide energy range, by hydrogenic Stark-effect calculations. This result is a consequence of the approximately hydrogenic behavior of the Stark components of rubidium at large fields. The onset of the continuum component in the cross section occurs at the "classical field-ionization threshold." This threshold is of importance only in systems which are not purely Coulombic (like rubidium), and gives rise to a minimum ionization rate for all levels with energies greater than this value.

(iii) The concept of "strong-field mixing" which is useful near $E = 0$ for Coulomb plus electric potential, is seen to merge naturally with a conventional perturbation calculation involving zero-field basis states at lower energies. Making use of both techniques allows tentative identification of most of the structure in the photoionization cross section.

ACKNOWLEDGMENTS

We wish to thank G. C. Bjorklund for many stimulating discussions concerning all aspects of this work, and D. Kleppner, K. T. Lu, and A. R. P. Rau for helpful comments.

[1] A. R. P. Rau, Phys. Rev. A 16, 613 (1977).
[2] A. R. Edmonds, J. Phys. (Paris) Colloq. 31, C4-71 (1970); A. F. Starace, J. Phys. B 6, 585 (1973); R. F. O'Connell, Astrophys. J. 187, 275 (1974); K. T. Lu, F. S. Tomkins, and W. R. S. Garton, Proc. R. Soc. Lond. A 364, 421 (1978); H. Crosswhite, U. Fano, K. T. Lu, and A. R. P. Rau, Phys. Rev. Lett. 42, 963 (1979).
[3] R. F. O'Connell, Phys. Rev. A 17, 1984 (1978); Phys. Lett. A 60, 481 (1977); M. G. Littman, M. M. Kash, and D. Kleppner, Phys. Rev. Lett. 41, 103 (1978); A. R. P. Rau, Ref. 1.
[4] W. R. S. Garton and F. S. Tomkins, Astrophys. J. 158, 839 (1969).
[5] F. A. Jenkins and E. Segre, Phys. Rev. 55, 52 (1939); C. D. Harper and M. D. Levenson, Opt. Commun. 20, 107 (1977); R. J. Fonck, F. L. Roesler, D. H. Tracy, K. T. Lu, F. S. Tomkins, and W. R. S. Garton, Phys. Rev. Lett. 39, 1513 (1977); M. L. Zimmerman, J. C. Castro, and D. Kleppner, Phys. Rev. Lett. 40, 1083 (1978); R. J. Fonck, D. H. Tracy, D. C. Wright, and F. S. Tomkins, Phys. Rev. Lett. 40, 1366 (1978); N. P. Economou, R. R. Freeman, and P. F. Liao, Phys. Rev. A 18, 2506 (1978); K. T. Lu, F. S. Tomkins, H. M. Crosswhite, and H. Crosswhite, Phys. Rev. Lett. 41, 1034 (1978).
[6] P. Jacquinot, S. Lieberman, and J. Pinard, Centre National de la Reserche Scientifique, Report No. 273 (1977) (unpublished); S. Feneuille, S. Lieberman, J. Pinard, and P. Jacquinot, C. R. Acad. Sci., Ser. B 284, 291 (1977).

[7]R. R. Freeman, N. P. Economou, G. C. Bjorklund, and K. T. Lu, Phys. Rev. Lett. 41, 1463 (1978).
[8]See, for example, D. S. Bailey, J. R. Hiskes, and A. C. Riviere, Nucl. Fusion 5, 41 (1965).
[9]See, for example, T. Yamabe, A. Tachibana, and H. J. Silverstone, Phys. Rev. A 16, 877 (1977).
[10]Littman, *et al.*, Ref. 3.
[11]S. Feneuille and P. Jacquinot, *Atomic Physics* (Plenum, New York, 1979), Vol. 6.
[12]E. Luc-Koenig and A. Bachelier, Phys. Rev. Lett. 43, 921 (1979).
[13]A. R. P. Rau (private communication) and J. Phys. B 12, L193 (1979).
[14]K. T. Lu (private communication).
[15]H. A. Bethe and E. E. Salpeter, *Quantum Mechanisms of One- and Two-Electron Atoms* (Springer-Verlag, Berlin, 1957).
[16]L. D. Landau and E. M. Lifshitz, *Quantum Mechanisms Non-Relativistic Theory* (Pergamon, London, 1958).
[17]A. R. P. Rau, J. Phys. B 12, L193 (1979).
[18]See R. F. O'Connell, Ref. 3.
[19]C. C. Grimes, T. R. Brown, M. L. Burns, and C. L. Zipfel, Phys. Rev. B 13, 140 (1976).
[20]J. D. Bekenstein and J. B. Kreiger, Phys. Rev. 188, 130 (1969); J. O. Hirschfelder and L. A. Curtiss, J. Chem. Phys. 55, 1395 (1971).
[21]P. M. Koch, Phys. Rev. Lett. 41, 99 (1978).